21st Australasian Fluid Mechanics Conference
Adelaide, Australia
10-13 December 2018

Numerical Study of the Transition of a Buoyant Plume from a Three-dimensional Open Cavity Heated from Below

M. Qiao[1], Z. Tian[2] and F. Xu[1]
[1]School of Civil Engineering
Beijing Jiaotong University, Beijing 100044, China

[2]Department of Mechanical Engineering
University of Adelaide, Adelaide, South Australia 5005, Australia

Abstract

The transition of a buoyant plume from an open cavity heated from below is studied by using numerical simulation. A small range of Rayleigh numbers from 10^4 to 10^5 and aspect ratio of A = 1/2, and Prandtl number of Pr = 0.7 (air) is considered. The plume from an open cavity heated below approaches a periodic puffing state around the Rayleigh number 8.6×10^4, it suggests that the plume from the open cavity heated below undergoes a supercritical Hopf bifurcation from a steady flow to a periodic flow. The following results reveal that there exists a series of period-doubling bifurcations after the Rayleigh number exceeds 8.6×10^4. Moreover, the phase pictures are displayed to understand the period-doubling bifurcations further. The understanding of the transition of buoyant plumes from a three-dimensional open cavity is of practical importance for the design of various systems such as smoke exhausts.

Nomenclature:

A	aspect ratio, H/D
B	bottom of the computational domain
D	diameter of the open cavity
g	acceleration due to gravity
H	height of the open cavity
k	thermal conductivity
Pr	Prandtl number, ν/κ
Ra	Rayleigh number, $g\beta\Delta TD^3/\nu\kappa$
t	time
t_0	initial time
Δt	time step
T	temperature
T_h	temperature of the heated bottom
T_0	initial temperature of the ambient fluid
u	x-velocity
v	y-velocity
w	z-velocity
x, y, z	nondimensional coordinate
β	coefficient of thermal expansion
κ	thermal diffusivity
ν	kinematic viscosity
ρ	density

Introduction

Natural convection is widely found in nature and industry [1-4]. Natural convection may rise from volcanoes, building ventilation, chimney, which is also referred to as plume. A plume is a fluid motion which is driven purely by continuous buoyancy sources. As a common type of natural convection, plumes are rapidly gaining attention in the research area due to their fundamental significance in a myriad of industrial and environmental flows [5-7].

Plumes could be laminar, transitional or turbulent. Laminar plumes exhibit a straight column in which the distribution of the temperature and the velocity is characterized in [8,9]. As for the transitional plume, the successively periodic vortical structures of transitional plumes on a heated plate were visualized in [10,11]. It was found that the onset of the transition of plumes occurs when the fluctuation appears downstream [12,13]. According to [14], the transition from a laminar to a turbulent plume passes through a sequence of bifurcations in a spatial temporal system. Apart from laminar and transitional plumes, turbulent plumes rising from a heat source were investigated [15-19]. Clearly, the classic plume theory solutions provide a reliable option to describe complex turbulent plumes [13,14]. Many studies (see e.g., [19]) have focused on entrainment of turbulent plumes. It was found that direct numerical simulation (DNS) is an appropriate method to characterize fine structures of entrainment and three-dimensional vortices of turbulent plumes. Entrainment is time-dependent in nature. This includes the contraction and expulsion phases in the ascent of turbulent plumes, which were captured using particle imaging velocimetry (PIV) technique [15].

The shape of the heat source plays a significant role in influencing the flow dynamics of plumes [20-22]. Experimental visualization showed that the heated fluid flows to the center of a heated plate and then ascends resulting in a plume [23]. The shape of the heated plate plays a role in the local heat transfer [20]. The dependence on governing parameters, such as the Rayleigh number, of the heat transfer of plumes rising from shape-different heated plates was quantified [22,23]. Furthermore, the heat transfer of laminar plumes on a heated plate with different extensions and restrictions was investigated [24-26].

The existing literature is almost devoid of studies pertaining to transitional plumes on a heat source of a non-ideal shape (except for a point, a line or a plane). In this study, we consider a plume arising from an open cavity heated from below, which serves as the basis for the understanding of the transition of natural convection flows and is of practical importance for the design of various systems such as smoke exhausts. A sequence of period-doubling bifurcations in the transition from a steady flow to an unsteady plume, with the increase of the Rayleigh number, is characterized.

Numerical procedure

The studies in [27-29] show that numerical simulation is capable of describing the transition of natural convection flows in a cavity. The three dimensional computational domain of $5\times5\times10$ is considered, as shown in Fig. 1. The open cavity of height H and diameter D is heated from below, and the bottom is maintained at a temperature of T_h. The sidewalls of the open cavity are assumed as adiabatic. At $t = 0$, the working fluid (air) is quiescent and the temperature is T_0. Natural convection flows inside and outside the open cavity are governed by the non-dimensional Navier-Stokes and temperature equations with the Boussinesq approximation as follows,

$$\frac{\partial u}{\partial x}+\frac{\partial v}{\partial y}+\frac{\partial w}{\partial z}=0, \tag{1}$$

$$\frac{\partial u}{\partial t}+u\frac{\partial u}{\partial x}+v\frac{\partial u}{\partial y}+w\frac{\partial u}{\partial z}=-\frac{\partial p}{\partial x}+\frac{\mathrm{Pr}}{\mathrm{Ra}^{1/2}}\left(\frac{\partial^2 u}{\partial x^2}+\frac{\partial^2 u}{\partial y^2}+\frac{\partial^2 u}{\partial z^2}\right), \tag{2}$$

$$\frac{\partial v}{\partial t}+u\frac{\partial v}{\partial x}+v\frac{\partial v}{\partial y}+w\frac{\partial v}{\partial z}=-\frac{\partial p}{\partial y}+\frac{\mathrm{Pr}}{\mathrm{Ra}^{1/2}}\left(\frac{\partial^2 v}{\partial x^2}+\frac{\partial^2 v}{\partial y^2}+\frac{\partial^2 v}{\partial z^2}\right), \tag{3}$$

$$\frac{\partial w}{\partial t}+u\frac{\partial w}{\partial x}+v\frac{\partial w}{\partial y}+w\frac{\partial w}{\partial z}=-\frac{\partial p}{\partial z}+\frac{\mathrm{Pr}}{\mathrm{Ra}^{1/2}}\left(\frac{\partial^2 w}{\partial x^2}+\frac{\partial^2 w}{\partial y^2}+\frac{\partial^2 w}{\partial z^2}\right)+\mathrm{Pr}T, \tag{4}$$

$$\frac{\partial T}{\partial t}+u\frac{\partial T}{\partial x}+v\frac{\partial T}{\partial y}+w\frac{\partial T}{\partial z}=\frac{1}{\mathrm{Ra}^{1/2}}\left(\frac{\partial^2 T}{\partial x^2}+\frac{\partial^2 T}{\partial y^2}+\frac{\partial^2 T}{\partial z^2}\right), \tag{5}$$

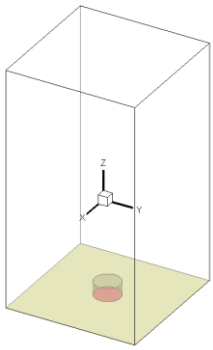

Figure 1. Sketch of the computational domain.

where u, v and w are the velocity components in the x, y and z directions respectively, t is time, T is the temperature, p is the pressure. The quantities are normalized using the following scales: $x, y, z \sim H$; $t \sim D^2/(\kappa \mathrm{Ra}^{1/2})$; $(T - T_0) \sim (T_h - T_0)$; $u, v, w \sim (\kappa \mathrm{Ra}^{1/2})/D$; and $\rho^{-1}\partial p/\partial x, \rho^{-1}\partial p/\partial y, \rho^{-1}\partial p/\partial z \sim \kappa^2 \mathrm{Ra}/D^3$. The dimensionless parameters in the governing equations and boundary conditions are the Rayleigh number, $\mathrm{Ra} = g\beta(T_h - T_0)D^3/\nu\kappa$, the Prandtl number, $\mathrm{Pr} = \nu/\kappa$, and the aspect ratio, $A = H/D$, in which g, H, D, T_0, T_h, β, ν and κ are acceleration due to gravity, the height and diameter of the open cavity, the initial temperature of the ambient fluid, the temperature of the heated bottom, coefficient of thermal expansion, viscosity, and thermal diffusivity, respectively.

A finite volume SIMPLE algorithm is used to implicitly solve the governing equations. A QUICK scheme is employed to discretize the advection term, and a second-order difference method is applied for the time integration (see [30] for details).

Mesh and the time step test		
Time step	**Mesh**	Variation of temperature at point (0, 0, -4.5)
0.042	5200 × 115	-
0.021	5200 × 115	1.0%
0.042	7400 × 160	1.1%

Table 1. Dependence test of the mesh and the time step.

The mesh is non-uniform in this study. That is, care is taken in sensitive areas where the element density increases because velocity and temperature gradients are more profound in these areas namely, near the bottom and sidewalls of the open cavity. The two meshes ($B \times H$) of 5200 × 115 and 7400 × 160 and the two time steps of 0.01 and 0.02 were tested pertaining to the maximum Rayleigh number ($\mathrm{Ra} = 10^6$). To quantify the effect of the mesh and time step on the plume from the open cavity, the difference between the average values of the temperatures at the fully developed state from t = 5000 to 9000 based on the two grids 5200 × 115 and 7400 × 160 is 1.1%, as shown in Table 1. Accordingly, to ease computational burden and time, the mesh of 5200 × 115 is adopted. Additionally, a time-step dependence analysis is conducted by using the dimensionless time-steps of 0.042 and 0.021. The difference of the average temperatures in the fully developed stage calculated using different time steps is 1.1%. This means that either of the two time-steps can be used. Considering the computing cost, the time-step of 0.042 is adopted (in which the Courant number is smaller than 0.5).

Results and discussion

The examination of results shows that the plume from the open cavity is steady with the increase of the Rayleigh number until $\mathrm{Ra} = 8.5 \times 10^4$. However, the plume becomes unsteady for $\mathrm{Ra} = 8.6 \times 10^4$, which is periodic puffing. That is, the transition from a steady to a periodic state occurs between $\mathrm{Ra} = 8.5 \times 10^4$ and 8.6×10^4, which is a Hopf bifurcation in which the oscillatory solution bifurcates from the steady solution as the Rayleigh number increases through a critical value.

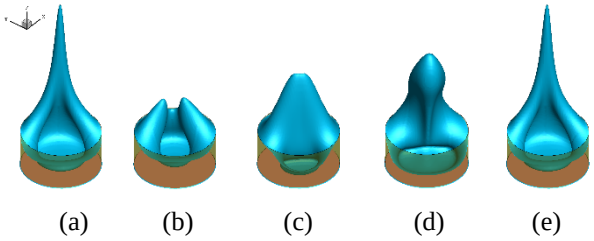

Figure 2. Isotherm (T = 0.25) for $\mathrm{Ra} = 9.4 \times 10^4$ at (a) $t = t_0$, (b) $t = t_0 + 4$, (c) $t = t_0 + 12$, (d) $t = t_0 + 18.2$ and (e) $t = t_0 + 24.6$.

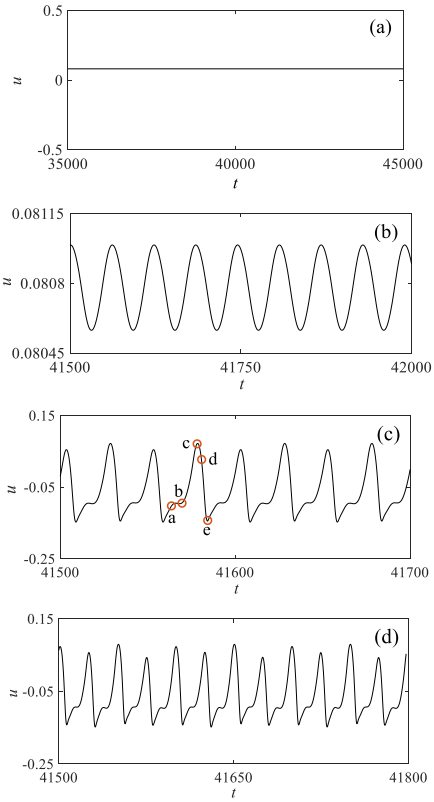

Figure 3. Time series of the x-velocity at the point (0, -4.75) at the steady or the periodic state. (a) $\mathrm{Ra} = 8.5 \times 10^4$. (b) $\mathrm{Ra} = 8.6 \times 10^4$. (c) $\mathrm{Ra} = 9.4 \times 10^4$. (d) $\mathrm{Ra} = 9.6 \times 10^4$.

Figure 2 shows isotherms over a puffing cycle within the non-dimensional time of 24.6 for Ra = 9.4×10^4. According to figure 2, at $t = t_0$, a polar plume appears from the open cavity, subsequently becomes weak, and separates to two polar plumes, as shown in figure (b). At the $t = t_0 + 12$, the two polar plumes are becoming strong again and a puff is detached from the open cavity at $t = t_0 + 24.6$, as displayed in figure2 (d). Finally, the two polar plumes merge.

A time series of the *x*-velocity at the point (0, 0, -4.75) is plotted in figure3 from (a) to (d) in order to better understand the Hopf bifurcation and subsequent period-doubling bifurcations. Clearly, the plume from the open cavity is steady for Ra = 8.5×10^4 and thus the value of the *x*-velocity at the point (0, 0,-4.75) approaches constant eventually. But the *x*-velocity is oscillatory for Ra = 8.6×10^4 as shown in figure2 (b). This means that the critical value of the transition from a steady to a periodic state lies between 8.5×10^4 and 8.6×10^4. The first period-doubling bifurcation occurs around Ra = 9.4×10^4. There are two repeating continuous waves with time, as shown in figure2 (c). The second period-doubling is found around Ra = 9.6×10^4, as shown by the replication of four continuous waves in figure2 (d). It is believed that infinite period-doubling bifurcations may occur before the plume from the open cavity become chaos.

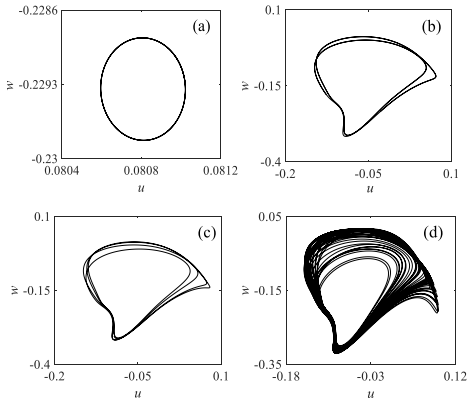

Figure 4. Phase space trajectories of *x*-velocity versus the *w*-velocity at the point (0, 0, -4.75) for (a) Ra = 8.6×10^4. (b) Ra = 9.4×10^4. (c) Ra = 9.6×10^4. (d) Ra = 1.1×10^5.

To describe a series of period-doubling bifurcations, the phase space trajectory of the *x*-velocity against the *w*-velocity is given in figure 4. As discussed above, the Hopf bifurcation occurs around Ra = 8.6×10^3 and thus a limit cycle is shown in figure4 (a). Figure 4 (c) is a closed curve and lies on a T^2 torus around Ra = 9.4×10^4, which is the first period-doubling bifurcation. Figure 4(d) displays the phase space trajectory lying on a T^4 torus for Ra = 9.6×10^4 after the second period-doubling bifurcation. The attractor in the figure4 (d) presents an infinite number of tori for Ra = 1.1×10^5 after a succession of period-doubling bifurcations.

Conclusions

The plume from the open cavity heated below appears periodic puffing when the Rayleigh number reaches Ra = 8.6×10^4. As the Rayleigh number increases further, a succession of period-doubling bifurcations occur. In addition, the attractor is presented for better depicting period-doubling bifurcations.

Acknowledgments

The authors would like to thank the National Natural Science Foundation of China (11572032), the 111 Project (B13002) for their financial support.

The authors would also like to acknowledge with great thanks to Phoenix support team, University of Adelaide, for supporting this simulation work.

References

[1] Morton, B.R., Forced plumes, *J. Fluid Mech*., **5**, 1959, 151-163.

[2] List, E. J., Turbulent jets and plumes, Annu. Rev. Fluid Mech., **14**, 1982, 189-212.

[3] Fay, J. A., Buoyant plumes and wakes, *Annu. Rev. Fluid Mech.*, **5**, 1973, 151-160.

[4] Gebhart, B., Instability, transition, and turbulence in buoyancy-induced flows, *Annu. Rev. Fluid Mech*., **5**, 1973, 213-246.

[5] Turner, J.S., Buoyant plumes and thermals, *Annu. Rev. Fluid Mech.*, **1**, 1969, 29-44.

[6] Woods, A.W., Turbulent plumes in nature, *Annu. Rev. Fluid Mech.*, **42**, 2010, 391-412.

[7] J.S. Turner, Turbulent entrainment: the development of the entrainment assumption, and its application to geophysical flows, *J. Fluid Mech.*, **173**, 1986, 431-471.

[8] Fujii T., Theory of the steady laminar natural convection above horizontal line heat source and a point source, *Int. J. Heat Mass Transf.*, **6**, 1963, 597-606.

[9] Kimura, S. & Bejan, A., Mechanism for transition to turbulence in buoyant plume flow, *Int. J. Heat Mass Transf.*, **26**, 1983, 1515-1532.

[10] Hattori, T., Norris, S.E., Kirkpatrick, M.P. & Armfield, S.W., Experimental and numerical investigation of unsteady behaviour in the near-field of pure thermal planar plumes, *Exp. Therm. Fluid Sci.*, **46**, 2013, 139-150.

[11] Jiang, X & Luo, K.H., Direct numerical simulation of the puffing phenomenon of an axisymmetric thermal plume, *Theoret. Comput. Fluid Dyn.*, **14**, 2000, 55-74.

[12] Pera, L. & Gebhart, B., On the stability of laminar plumes: some numerical solutions and experiments, *Int. J. Heat Mass Transf.*, **14**, 1971, 975-984.

[13] Bill, R.G. & Gebhart, B., The transition of plane plumes, *Int. J. Heat Mass Transf.*, **18**, 1975, 513-526.

[14] Lopez, J.M. & Marques, F., Instability of plumes driven by localized heating, *J. Fluid Mech.*, **736**, 2013, 616-640.

[15] Vouros, A. & Panidis, T., Statistical analysis of turbulent thermal free convection over a horizontal heated plate in an open top cavity, *Exp. Therm. Fluid Sci*., **36**, 2012, 44-55.

[16] Ezzamel, A., Salizzoni, P. & Hunt, G.R., Dynamical variability of axisymmetric buoyant plumes, *J. Fluid Mech*., **765**, 2015, 576-611.

[17] Hunt, G.R. & Van Den Bremerk, T.S., Classical plume theory: 1937-2010 and beyond, *J. Appl. Math.* **76**, 2011, 424-448.

[18] Kaye, N.B., Turbulent plumes in stratified environments: a review of recent work, *Atmos. Ocean*, **46**, 2008, 433-441.

[19] Plourde, F., Pham, M.V., Kim, S.D. & Balachandar, S., Direct numerical simulations of a rapidly expanding

thermal plume: structure and entrainment interaction, *J. Fluid Mech*., **604**, 2008, 99-123.

[20] Husar, R.B. & Sparrow, E.M., Patterns of free convection flow adjacent to horizontal heated surfaces, *Int. J. Heat Mass Transf.*, **11**, 1968, 1207-1208.

[21] Sparrow, E.M., Husar, R.B. & Goldstein, R.J., Observations and other characteristics of thermals, *J. Fluid Mech.*, **41**, 1970, 793-800.

[22] Lloyd, J.R. & Moran, W.R., Natural convection adjacent to horizontal surfaces of various planforms, *Trans. ASME. J. Heat Transf.*, **96**, 1974, 443-447.

[23] Kitamura, K., Mitsuishi, A., Suzuki, T. & Kimura, F., Fluid flow and heat transfer of natural convection adjacent to upwardfacing plates of arbitrary aspect ratios, *Int. J. Heat Mass Transf.*, **89**, 2015, 320-332.

[24] Goldstein, R.J. & Lau, K.S., Laminar natural convection from a horizontal plate and the influence of plate-edge extensions, *J. Fluid Mech.* **129**, 1983, 55-75.

[25] Saha, S.C. & Gu, Y.T., Transient air flow and heat transfer in a triangular enclosure with a conducting partition, *Appl. Math. Model.*, **38**, 2014, 3879-3887.

[26] Saha, S.C., Khan, M.M.K. & Gu, Y.T., Unsteady buoyancy driven flows and heat transfer through coupled thermal boundary layers in a partitioned triangular enclosure, *Int. J. Heat Mass Transf*., **68**, 2014, 375-382.

[27] Bastiaansa, R.J.M., Rindta, C.C.M., Nieuwstadt, F.T.M. & Steenhoven, A.A.V., Direct and large-eddy simulation of the transition of two-and three-dimensional plane plumes in a confined enclosure, *Int. J. Heat Mass Transf*., 43, 2000, 2375-2393.

[28] Lombardi, M., Caulfield, C.P., Cossu, C., Pesci, A.I. & Goldstein, R.E., Growth and instability of a laminar plume in a strongly stratified environment, *J. Fluid Mech*., **671**, 2011, 184-206.

[29] Oteski, L., Duguet, Y. & Pastur, L.R., Lagrangian chaos in confined two-dimensional oscillatory convection, *J. Fluid Mech.*, **759**, 2014, 489-519.

[30] Qiao, M., Xu, F. & Saha, S.C., Scaling analysis and numerical simulation of natural convection from a duct, *Numer. Heat Transf. Part A*, **72**, 2017, 355-371.